Journal of Network Intelligence
Taiwan Ubiquitous Information
 ISSN 2414-8105 (Online)
Volume **8**, Number **1**, February **2023**

Motor Torque Compensation Control Strategy of Pure Electric Bus Based on Fuzzy Reasoning

Gui-Bin Sun

School of Mechanical and Automotive Engineering,
Xiamen University of Technology,
Fujian Key Laboratory of Advanced Design and Manufacture for Bus,
Xiamen, 361024, Fujian Province, China
sgbzxx@xmut.edu.cn

Shen Zhou

School of Mechanical and Automotive Engineering,
Xiamen University of Technology,
Xiamen, 361024, Fujian Province, China
2022031369@s.xmut.edu.cn

Yi-Jui Chiu*

School of Mechanical and Automotive Engineering,
Xiamen University of Technology,
Xiamen, 361024, Fujian Province, China
chiuyijui@xmut.edu.cn

Wen-De Zhuo

Xiamen Fengtai International New Energy Vehicle Co.,
Xiamen, 361024, Fujian Province, China
945925413@qq.com

Sheng-Rui Jian

Department of Materials Science and Engineering,
I-Shou University,
Kaohsiung 84001, Taiwan
Department of Applied Physics,
National University of Kaohsiung,
Kaohsiung 81148, Taiwan
srjian@isu.edu.tw

*Corresponding author: Yi-Jui Chiu
Received September 2, 2022, revised October 17, 2022, accepted December 4, 2022.

Abstract. *Pure electric buses play an important role in energy conservation, emission reduction and transportation. However, pure electric buses start slowly because they have low power relative to their large mass, and they do not handle comfortably. Aiming to solve the power and comfort problems of pure electric buses, the ability of the bus to be controlled by the driver is optimized in this study. The motor control strategy is studied to improve the driver demand for pure electric buses. First, the dynamics and torque distribution of three accelerator pedal control strategies are discussed in this paper. A control strategy based on the equal proportion accelerator pedal is proposed. The control strategy aims to meet the driver's needs. According to expert experience, a rule is formulated to meet the driver's needs based on the driver's control of the accelerator pedal. Second, a MATLAB/Simulink model is built and a step function is used as the accelerator aperture to simulate the start of acceleration in order to verify the developed strategy. The simulation results show that the control strategy increases the starting response time by 51.7 %. Then, the control strategy is imported to the vehicle controller for real vehicle experiments, and the output torque, throttle pedal opening and throttle opening change rate data are obtained from the vehicle controller. Finally, the experimental results show that the starting response time of a pure electric bus increases by* 44.44% *and the acceleration response time increases by* 62.86% *during driving when using the control strategy. The response time is reduced by* 0.80*s for the first deceleration and by* 0.62*s for the second deceleration. The results are consistent with the rules and can meet the needs of drivers. Therefore, the proposed motor torque compensation control strategy could significantly reduce the response time and meet the driver's torque requirement for pure electric buses.*
Keywords: pure electric buses; driving demand; control strategy; torque compensation control strategy

1. **Introduction.** Due to their convenience and zero emissions, pure electric vehicles (PEVs) are widely welcomed. The comfort and handling of PEVs directly affect the promotion of PEVs. In a study on vehicle energy consumption economy, Wu et al. [1] investigated the in-wheel motor of PEVs and found that the traditional torque distribution strategy is not suitable for four-wheel in-wheel motor vehicles. A torque power distribution method was proposed for power optimization. The simulation results showed that the driving range increased and the energy consumption decreased compared with the traditional torque average distribution strategy of electric vehicles under different working conditions. Qi [2], aiming to solve the problem of acceleration and efficiency of energy of vehicles on urban roads, developed a fuzzy controller suitable for driver's intention by using a fuzzy control algorithm. It was found that the controller could improve the response speed of PEVs, efficiently recover braking energy, and satisfy the driver's requirement for acceleration. Chen et al. [3] studied the braking energy recovery and body stability of PEVs. They utilized the NSGA-II algorithm to carry out multi-objective optimization for stability and braking energy recovery, and they established a vehicle power model and an energy regeneration system. The simulation results showed that the stability and energy recovery efficiency were improved after optimization. The aforementioned studies improved the driving range of PEVs but did not consider power and comfort. Power, energy consumption economy and comfort are all important indicators of vehicle performance and should all be considered.

Considerable research has been carried out on the influence of mode switching on vehicle performance. Zeng et al. [4] studied the optimization of torque fluctuation of hybrid vehicles when switching the working mode. A rule control strategy was proposed for dividing the working range of hybrid vehicles. The torque of the motor and engine were distributed and a power model was established. The team found the proposed control

method could reduce the vehicle torque fluctuation in simulations. The results of experiments were consistent with the simulation results, demonstrating that the proposed method is feasible. Ding et al. [5] found that the process of changing from pure electric mode to motor mode is related to vehicle power and driving ability, so it affects the driver's driving experience. The team studied fast and stable optimization in the working mode conversion process of hybrid vehicles. In order to obtain the target torque trajectory of the transmission, the team designed a new strategy and optimized target parameters by particle swarm optimization. According to simulations, the mode switching process became fast and stable under the proposed control method, which means the driving quality was improved. Chen et al. [6] designed three manually selected modes to meet the driver's acceleration intention and selected different optimization objects in the three modes. The simulation results showed that the designed manual mode could meet the expectation of driving acceleration intention. Yang et al. [7] studied the problem of vehicle jitter caused by torque fluctuation during mode switching of PEVs with multiple braking modes. The team proposed a comprehensive control method for vehicle braking. The stability of braking mode switching was realized by driver braking intention and motor braking force compensation. The simulation results showed that the torque fluctuation was reduced in the process of braking mode conversion. Xiao et al. [8] designed a coordinated control strategy in which the driving motor participates in the shift process, which aims to shorten the shift time of two gear automated mechanical transmission PEVs and ensure smooth shift. The team carried out simulation and experiments on the proposed strategy. Both results showed that the proposed strategy could meet the expectations for shift time and stability. Chen et al. [9] found that torque vibration will affect the performance of the transmission system. An active control strategy was proposed to suppress torque vibration, and it was found that the proposed control method could reduce torque vibration and interference from simulation results. PEVs have only one working mode. Hence, it is unnecessary to consider the impact of switching the working mode of PEVs based on comfort. Comfort is indispensable for PEVs, and power performance is also an important indicator of PEVs. However, the above study did not take into account whether the power performance of the heavy-duty vehicle met the requirements of the driver. Power performance is an important index of overall pure electric bus performance.

For the optimization of power performance of PEVs, Mo et al. [10] studied the robustness of PEVs on a ramp and proposed to use the incremental proportional-integral (PI) algorithm starting controller to achieve the target speed. By comparing the simulation results of the proposed control method with the experimental results of the traditional control strategy, it was found that the designed control method was fast and stable in the process of mode switching, meaning it could improve driving quality. Zhang et al. [11] worked to reduce torque ripple and complexity. The team analyzed and improved the model predictive torque control (MPTC). Compared with traditional MPTC, the experimental results showed that the improved MPTC still had short response time like traditional MPTC, but the stability was improved and the torque ripple was reduced. Deng et al. [12] proposed a power performance optimization strategy for driver intention recognition. It was different from the traditional PEV power mode, as it could optimize the power and handling at the same time. It was found that the improved vehicle performance could meet the driver's expectations through simulation. Yang [13] analyzed the current characteristics of vehicle acceleration and proposed a power coupling drive system in which hydraulic energy, electric energy and mechanical energy could be converted to each other. Simulation results showed that the acceleration performance was improved by this system, and real vehicle experimental results showed that the speed could be controlled well and that the driving range increased. Xiong et al. [14] proposed an adaptive

dual-motor optimal torque control method for PEVs in which the motor torque was distributed and optimized according to the road conditions. Simulation results showed that the proposed method could reduce energy loss. Sun et al. [15] studied the three gear electric vehicle, matched the motor according to the vehicle parameters, and developed a dynamic gear shifting strategy. The simulation results show that the gear shifting strategy can improve motor efficiency. Shi et al. [16] studied the handing of dual-motor pure electric racing cars and proposed a control strategy conducive to vehicle handling and stability. Experimental results showed that the convergence speed of the car increased, and the handling stability improved. Lei et al. [17] proposed an intention classification and recognition method to realize adaptive decision-making and reflect the adaptive driving intention of vehicles. The experimental results show that the proposed method is effective. Ju et al. [18] proposed driving intention emergency braking and selected eigenvalues with different methods. The experimental results show that driving intention can be detected, and the system accuracy is high, which can meet the requirements of auxiliary driving. Liu et al. [19] established a driving intention prediction model using driver data. The experimental results show that it is conducive to the development of driving prediction. Lian et al. [20] put forward a direct inference method of driving intention. Hardware in the loop simulation demonstrates the safe driving intention is effective. Liu et al. [21] proposed a driving intention prediction method for traffic in mixed scenes to improve the safety of automatic driving. The experimental results show that the proposed method has higher accuracy. Liu et al. [22] proposed a recognition method to accurately identify driving intentions. The experimental results show that the proposed method is better at identifying driving intentions, which is of great significance for improving safety. Driving intention is mostly used in the field of assistant driving, and it is less involved in ensuring a vehicle meets the driver's needs, but it is still of great significance to study driving intention in vehicles. Li et al. [23] designed a fuzzy controller combining force distribution. The goal was to improve vehicle braking stability and energy recovery. It was indicated that simulation resulted in braking performance and comfort. The vehicle energy recovery efficiency was significantly improved. This paragrap is a study of the power performance of PEVs. PEVs are different from pure electric buses. Pure electric buses rely on a rich driving experience to ensure passengers have a good riding experience. None of research discussed above took into account the driving intention or vehicle power of the vehicles. Therefore, the power performance research of pure electric buses should be based on the driving intention. The driving intention and the power performance of pure electric buses should be comprehensively considered to achieve the goal of comfort.

The aforementioned studies investigated either comfort or power rather than taking these factors into account simultaneously, and they paid little attention to the driver. This paper proposes a control strategy for output torque based on fuzzy reasoning and driving intention, aiming to solve the power problem of PEVs. After analyzing three accelerator pedal torque control strategies, it is determined that the equal proportion pedal torque compensation control strategy is most suitable for formulating the driver's driving intention. Three membership functions are set corresponding to accelerator aperture, change rate of accelerator aperture and compensation coefficient of torque. Suitable fuzzy rules are designed, and the maximum membership function is used to defuzzificate. A MATLAB/Simulink model is created to test the proposed control strategy, and the simulation results show that the strategy is feasible. Finally, the practical experimental are carried out to further test the control strategy.

2. **Driver Demand Torque Analysis.**

The structure related to the drive motor of a pure electric bus is shown in Figure 1. Power battery, Vehicle Control Unit (VCU), Motor

Control Unit (MCU), driving motor and transmission device are included in Figure 1. The power battery supplies power to the system. The VCU receives signals and sends signals to the MCU to control the motor [24].

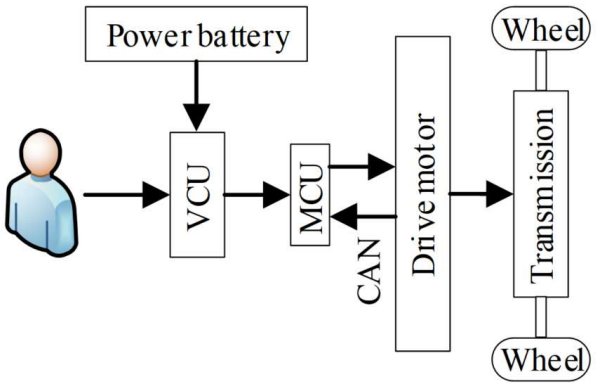

FIGURE 1. The structure related to the drive motor of a pure electric bus

At present, there are three common accelerator pedal torque control strategies: soft pedal torque control strategy, hard pedal torque control strategy and equal proportion pedal torque control strategy. Acceleration torque coefficient versus accelerator aperture curves corresponding to these three torque control strategies are displayed in Figure 2 [25].

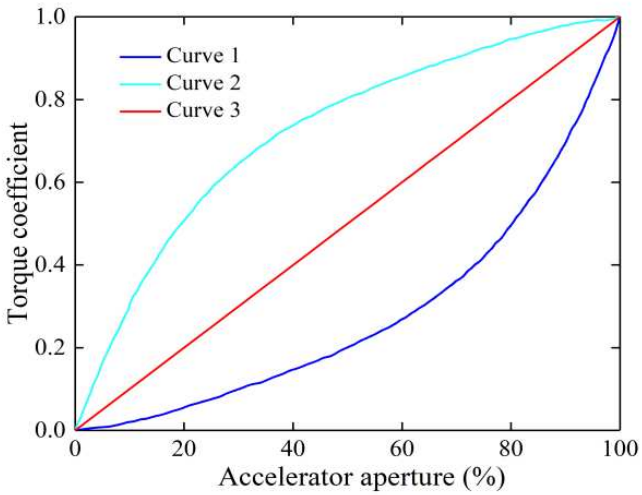

FIGURE 2. Acceleration torque versus accelerator aperture for three torque control strategies

Curve 1 corresponds to the soft pedal torque control strategy. The slope of Curve 1 increases gradually. The output torque with this strategy is small at small accelerator aperture, but the torque increases sharply with increasing accelerator aperture. This control strategy could provide the driver with better power experience under high accelerator aperture, but the vehicle will feel soft when first starting to accelerate. The low load handling of the vehicle will best with this strategy. Curve 2 corresponds to the hard pedal torque control strategy. The slope of Curve 2 decreases gradually. The output torque increases quickly at small accelerator aperture, and then more slowly under large

accelerator aperture. This strategy could provide drivers with a better power experience at medium and low loads, but the handling will not be ideal. Curve 3 corresponds to the equal proportion pedal torque control strategy. The slope of Curve 3 remains unchanged. The actual position of the accelerator pedal is reflected by the torque. The power experience and handling are between those of Curve 1 and Curve 2.

In Figure 2, the X-axis represents the accelerator aperture, which is in the range [0, 1], and the Y-axis represents the driving torque coefficient, which is in the range [0, 1]. MATLAB is used to fit the three curves. The corresponding functional relationships of the three curves are defined as $f_1(x)$, $f_2(x)$ and $f_3(x)$. The design of motor output demand torque is expressed as follows:

$$T_{dema} = \begin{cases} f_1(x)T_{N\_max}(N_{out}), n = 1 \\ f_2(x)T_{N\_max}(N_{out}), n = 2 \\ f_3(x)T_{N\_max}(N_{out}), n = 3. \end{cases} \tag{1}$$

where T_{dema} denotes the motor output demand torque, $T_{N\_\max}$ is the maximum allowable output torque of the motor in real time, N_{out} is the actual output speed of the motor and n (the subscript of f) identifies the torque control strategy by corresponding curve number.

2.1. **Torque Strategy Analysis.** The three-accelerator pedal torque control strategies are analyzed according to Equation (1). The distributions of throttle gradients corresponding to the three strategies are shown in Figure 3 [26]. The accelerator aperture distribution of the soft pedal torque control strategy is shown in Figure 3(a). It can be seen from Figure 3(a) that the distribution density of the accelerator aperture curve decreases with the increase in the motor output torque. The output torque changes little with the change of speed under small accelerator aperture. In terms of the driver's subjective perception, the power performance of the vehicle is poor when the accelerator aperture is small and improves as the accelerator aperture increases. The accelerator aperture distribution of the hard pedal torque control strategy is shown in Figure 3(b). The distribution density of the accelerator aperture curve increases with the increase in the motor output torque. In terms of the driver's subjective perception, even if the accelerator aperture is small, the vehicle has good power performance, and the power performance does not increase significantly with the increase of accelerator aperture. This strategy is more conducive to the rapid start of the vehicle, but it is more difficult for the driver to control the vehicle under the driving condition of small accelerator aperture. The accelerator aperture distribution of the equal proportion pedal torque control strategy is shown in Figure 3(c). The density of different accelerator aperture curves is evenly distributed. The power performance and handling of the vehicle at each stage are between those of the soft pedal and hard pedal torque control strategies.

2.2. **Select Torque Control Strategy.** According to the above analysis, the three accelerator pedal torque control strategies have their own advantages and disadvantages. Since the equal proportional pedal torque control strategy has better implementation and control in the VCU control program than the other two control methods, torque compensation in this paper is based on the equal proportion pedal torque control strategy. The torque compensation coefficient is determined by the driver's operation intention, taking into account the vehicle power demand and vehicle handling. The required driving torque is divided into two parts: reference torque and compensation torque. The reference torque is determined by the real-time accelerator aperture size and equal proportion pedal torque control strategy. The compensation torque is determined by the driver's driving

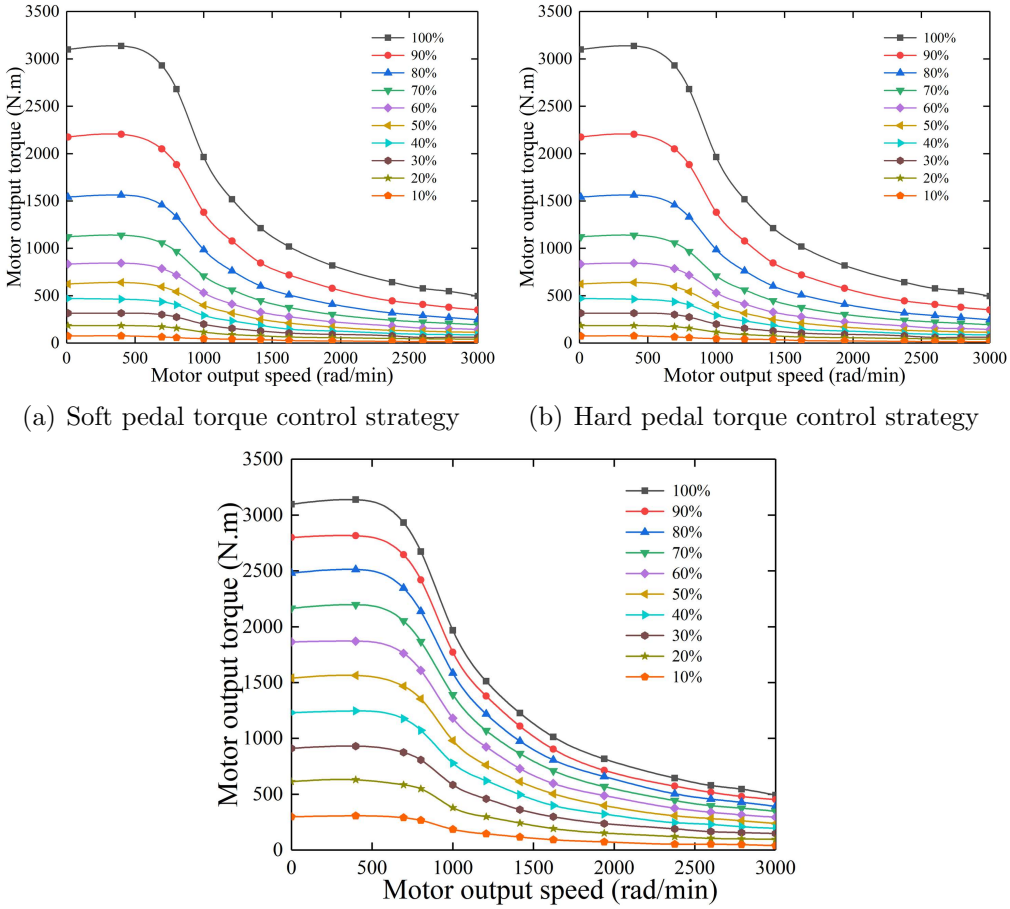

(a) Soft pedal torque control strategy

(b) Hard pedal torque control strategy

(c) Equal proportion pedal torque control strategy

FIGURE 3. Accelerator gradient distribution [26]

intention. The final demand torque is equal to the sum of the reference torque and the compensation torque. The final demand torque is expressed as follows:

$$T_{out\_need} = T_{dema} + T_{compen} \tag{2}$$

where T_{out_need} denotes the final demand torque, T_{dema} is the reference torque and T_{compen} is the motor output compensation torque.

The purpose of torque compensation is to meet the torque demand of the driver as soon as possible to reduce the acceleration or deceleration time while improving the handling and stability of the whole vehicle. The torque compensation is determined by the driving intention. The current accelerator aperture and the change rate of accelerator aperture are selected as inputs. The driving intention is judged through fuzzy reasoning. The torque compensation coefficient is obtained in the current driving state. The torque compensation coefficient is expressed as follows:

$$T_{compen} = T_{max} \cdot i_{Tmax\_Precen} \cdot i_{Acc} \tag{3}$$

where i_{Tmax_Percen} denotes the compensation torque limit coefficient, and i_{Acc} is the torque compensation coefficient.

2.3. **Determine Driving Intention.** The driving intention refers to the driver's intention to control the accelerator aperture and the change rate of the accelerator aperture according to their past driving experience under different motion conditions and road

conditions so as to achieve their desired vehicle power. Due to the characteristics of pure electric buses, the equal proportion pedal torque control strategy is used to reduce the operation pressure of VCU in this paper. The average change rate of accelerator aperture could only reflect the current state of the accelerator pedal. Therefore, based on the change rate of the accelerator aperture, the acceleration of the accelerator aperture is introduced. The acceleration of the accelerator aperture is calculated to predict the driving intention so as to achieve the purpose of torque compensation response as fast as possible. The change rate of the accelerator aperture of a pure electric bus is expressed as follows:

$$K_{Acc_i} = (Acc_i - Acc_{i-1})/T \tag{4}$$

where K_{Acc_i} denotes the change rate of accelerator aperture at the i-th sampling time point, Acc_i is the accelerator aperture at the i-th sampling time point, Acc_{i-1} is the accelerator aperture at the (i-1)-th sampling time point and T is the adoption period.

The acceleration of the accelerator aperture is expressed as follows:

$$a_i = \Delta K_{Acc_i}/\triangle T = (K_{Acc_i} - K_{Acc_i-1})/T \tag{5}$$

where a_i denotes the acceleration of the accelerator aperture at the i-th sampling time point.

The acceleration of the accelerator aperture is expressed as follows:

$$E(A) = \Sigma a_i/n, (i = 1, 2, \ldots, n) \tag{6}$$

where n denotes the adoption time from the first time point to the i-th time point.

The variance of the acceleration of the accelerator aperture is expressed as follows:

$$\sigma(A_{Acc}) = \sqrt{E[(a - E(a))^2]} \tag{7}$$

The current accelerator pedal state could be judged according to the acceleration of the accelerator aperture and variance of the acceleration of the accelerator aperture. The fuzzy database is queried so as to provide torque compensation tailored to the driving intention.

3. **Determination of Torque Compensation Coefficient and Simulation.** The current optimization algorithms are also diversified. Different algorithms are best suited for different optimization objectives. In the field of control, adaptive control is mostly used for high-precision models, focusing on the dynamic performance of the system. Predictive control is applicable to the application of multi input, multi output and constrained models, focusing on the overall steady-state performance of the system. Fuzzy control is applicable without a specific model, mainly based on experimental data and expert experience [27, 28]. The output torque is optimized by adding compensation torque, which is determined by the driver's requirements in this paper. The driver's requirements for torque are different in different states. The driver's torque requirements are uncertain, so the fuzzy reasoning algorithm is selected because it does not require exact data. The flowchart of fuzzy reasoning is shown in Figure 4. First the input signal is fuzzified, then the fuzzy inference is carried out according to the fuzzy rules, and finally the output control signal is defuzzified.

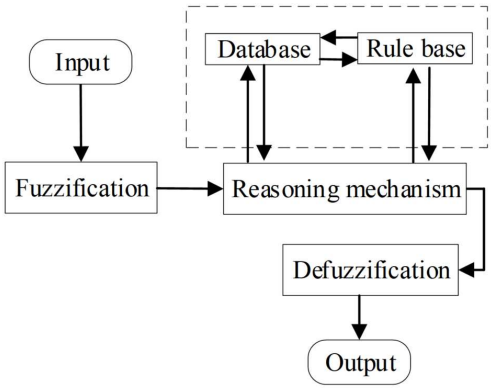

FIGURE 4. Flowchart of fuzzy reasoning

3.1. **Set Membership Degree Function.** Editing the membership degree function is an important part of fuzzy control since this function directly affects the output of the controller. Fuzzy statistics method, example method and expert experience method are commonly used to edit the input variables of membership degree functions. To make the torque meet the driver's expectation, the proposed motor torque control strategy is based on driving intention. Therefore, the expert experience method is used to design the membership degree function of input variables in this paper.

The input variables are defined, and Figure $5-7$ are drawn according to [29]. The domain of the accelerator aperture is [0, 1]. The fuzzy logic control strategy is designed according to the specific accelerator aperture size. The fuzzy subset of accelerator aperture is divided into zero, small, medium, large, maximum, namely $\{ZE, S, M, B, ZB\}$. Trimf Function is selected as the membership degree function. Equation (8) is the formula of Trimf Function (TRIF). The curve of accelerator aperture membership function is shown in Figure 5.

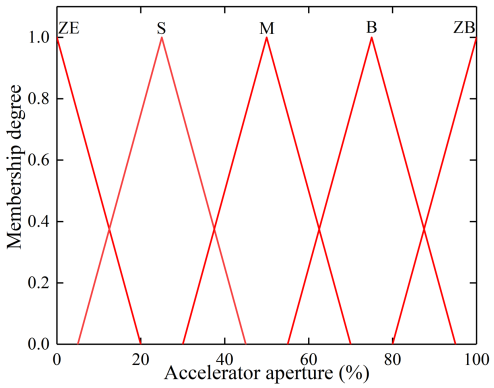

FIGURE 5. Membership degree function of accelerator aperture

$$f(x) = \begin{cases} \frac{x-a_1}{b-a_1}, a_1 \leq x \leq b_1 \\ \frac{c_1-x}{c_1-b}, b_1 \leq x \leq c_1 \end{cases} \tag{8}$$

where x denotes variable, and a_1, b_1 and c_1 are constants.

The domain of the change rate of accelerator aperture is set to [-100% , 100%]. The fuzzy subset of the change rate of accelerator aperture K_{Acc} is divided based on practical experience into negative big, negative middle, negative small, zero, positive small, positive middle, positive big, denoted as $\{NB, NM, NS, ZE, PS, PM, PB\}$. Trimf Function and

Trapmf Function are used to set the membership degree function of the change rate of accelerator aperture. Equation (9) is the formula of Trapmf Function (TRAF). The curve of the change rate of accelerator aperture is shown in Figure 6.

$$f(x) = \begin{cases} \frac{x-a_2}{b_2-a_2}, a_2 \le x \le b_2 \\ 1 \quad\quad , b_2 \le x \le c_2 \\ \frac{d-x}{d-c_2} \ , c_2 \le x \le d \end{cases} \tag{9}$$

where a_2, b_2, c_2 and d are constants.

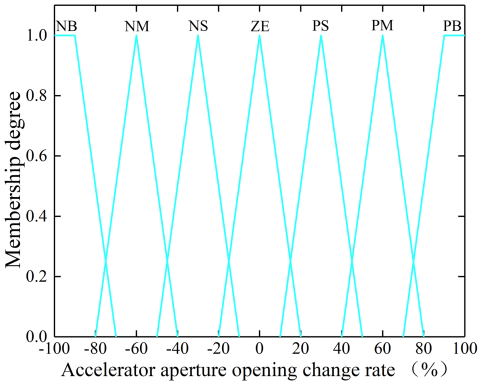

FIGURE 6. Membership degree function of change rate of accelerator aperture

The domain of torque compensation coefficient i_{Acc} is set to [-1, 1]. The torque compensation coefficient is divided into negative large, negative medium, negative small, zero, positive small, positive medium, positive large, denoted as $\{NB, NM, NS, ZE, PS, PM, PB\}$. It is similar to the membership degree function of the change rate of accelerator aperture. The Trimf Function and Trapmf Function are used to set the membership degree function of the torque compensation coefficient. The membership degree function of the torque compensation coefficient is shown in Figure 7.

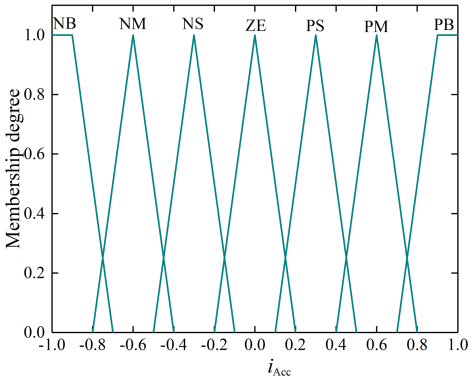

FIGURE 7. Membership degree function of torque compensation coefficient

3.2. **Set Fuzzy Rules and Defuzzification.** It can be seen from the fuzzy inference flowchart Figure 4 that the key of the inference mechanism is the fuzzy rule base. Fuzzy rules have a direct impact on the power, energy consumption economy and comfort of a vehicle. It is very important to formulate fuzzy control rules reasonably [30]. Fuzzy rules have no rules to follow, so they are mainly based on expert experience and experimental data. The fuzzy control rules proposed generally meet the driver's intention. When *Acc*

$= S$, to improve the controllability of the small throttle driving condition, no matter whether K_{Acc} is any fuzzy subset, no compensation will be made, and it is set that $i_{Acc} = ZE$. The greater the change rate of the accelerator pedal opening, the greater the driver's demand for torque. When $Acc = M$ and $K_{Acc} = PM$, it is set that $i_{Acc} = PM$, and i_{Acc} increases with the increase of K_{Acc}. The compensation should not be too large to control the vehicle handling. When $Acc = ZB$ and $K_{Acc} = PB$, it is set that $i_{Acc} = PM$. When the change rate of the accelerator opening is zero, it indicates that the driver's torque demand is unchanged. When $K_{Acc} = ZE$, Acc has no compensation, and it is set that $i_{Acc} = ZE$. When the change rate of the accelerator opening is less than zero, it indicates that the torque demand becomes small. When $Acc = ZB$ and $K_{Acc} = NS$, it is set that $i_{Acc} = NM$ and i_{Acc} decreases as K_{Acc} decreases. The rules are shown in Table 1.

Table 1. Fuzzy control rules

i_{Acc}	K_{Acc}						
Acc	NB	NM	NS	ZE	PS	PM	PB
ZE	ZE	ZE	ZE	ZE	ZE	ZE	ZE
ZE	NS	NS	ZE	ZE	PS	PM	PB
ZE	NM	NS	NS	ZE	PS	PM	PB
ZE	NB	NM	NS	ZE	PS	PS	PB
ZB	NB	NM	NM	ZE	ZE	PS	PM

The fuzzy rules of the membership degree function are set by using the fuzzy control tool in MATLAB according to the rules in Table 1. The driver controls the vehicle mainly by controlling the accelerator aperture and the change rate of the accelerator aperture according to the driver's requirement for torque. Therefore, in this paper, the accelerator aperture and the change rate of the accelerator aperture are defined as the inputs, and the torque compensation coefficient is defined as the output. The framework of the fuzzy reasoning is shown in Figure 8.

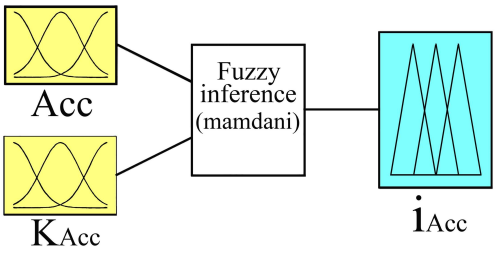

Figure 8. The framework of the fuzzy reasoning

The design of fuzzy rules is shown in Figure 9 according to the defined fuzziers of Acc, K_{Acc} and i_{Acc}. There are 35 fuzzy rules in this paper. The rule of the accelerator aperture is shown in Figure 9(a). Region a corresponds to ZE, region b corresponds to S, region c corresponds to M, region b corresponds to B and region c corresponds to ZB. Figure 9(b) shows the rule of the change rate of the accelerator aperture with seven triangles in region a. Subsets (NB, NM, NS, ZE, PS, PMandPB) are defined as different change rates of accelerator aperture from top to bottom in region a in Figure 9(b). Similarly, there are seven graphs in Figure 9(b) region b. Subsets (NB, NM, NS, ZE, PS, PM and PB) are defined as different change rates of accelerator aperture from top to bottom in region b in Figure 9(b). Figure 9(b) could be summarized as follows: region X in Figure 9(a) corresponds to region X in Figure 9(b). There are five regions in Figure 9(b), and

each region has seven triangles, corresponding to subsets (NB, NM, NS, ZE, PS, PM and PB) from bottom to bottom. In Figure 9(a), the red vertical bar indicates the value of the accelerator aperture in the tool window. In Figure 9(b), the red vertical bar indicates the value of the change rate of accelerator aperture defined in the tool window.

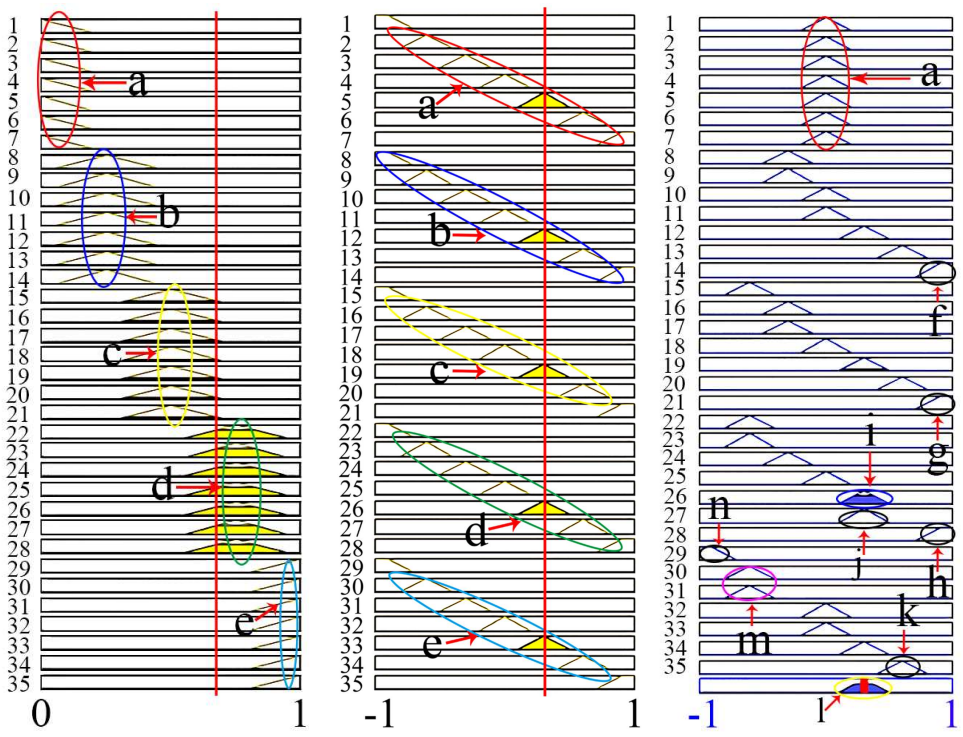

(a) Acc = 0.65 (b) $K_{Acc} = 0.307$ (c) $i_{Acc} = 0.3$

FIGURE 9. Fuzzy rule design

Region a of Figure 9(c) is distributed in the middle of the abscissa, and the compensation coefficient is zero at this time, indicating that there is no compensation. The region i is a blue triangle in Figure 9(c), indicating that the compensation coefficient is PS. The abscissa of region m and n are negative in Figure 9(c). At this time, they are represented as NB and NM, respectively. Region l in Figure 9(c) represents the value of defuzzification. All design rules and program are shown in Appendix A. For example, the accelerator aperture is defined as B, corresponding to region d in Figure 9(a), and the change rate of accelerator aperture is defined as PS, corresponding to region e in Figure 9(b). The output compensation coefficient of fuzzy controller is PS. The design achieves consistency with the actual driver's driving requirements by controlling the accelerator aperture and the change rate of the accelerator aperture.

The result of fuzzy reasoning is a fuzzy set. In the control field, the output is a certain value. Therefore, it is necessary to convert the fuzzy reasoning result into an accurate value. This process is called defuzzification. The maximum membership method, center of gravity method and weighted average method are three common methods of defuzzification. The maximum membership method does not consider the shape of the membership function, only the output value. The advantage is that the calculation is simple. Considering the limited computing power of VCU and the real-time performance of signal processing, the maximum membership method is used in this paper.

The largest element in the result is expressed as follows:

$$\bar{A}_i \in F(X), (i = 0, 1, 2, \ldots, n) \tag{10}$$

where X denotes all individuals of the element to be identified.

The membership function $\bar{\varphi}A_1(x)$,$\bar{\varphi}A_2(x)$,..., $\bar{\varphi}A_n(x)$ is set as the corresponding mode. Then the relationship is expressed as follows:

$$\bar{\varphi}A_l(x) = max\{\bar{\varphi}A_1(x), \bar{\varphi}A_2(x), \ldots, \bar{\varphi}A_n(x)\} \tag{11}$$

The Mamdani fuzzy inference method [31] is chosen in this paper. The fuzzy inference of the torque compensation coefficient is shown in Figure 10 according to the fuzzy control rules.

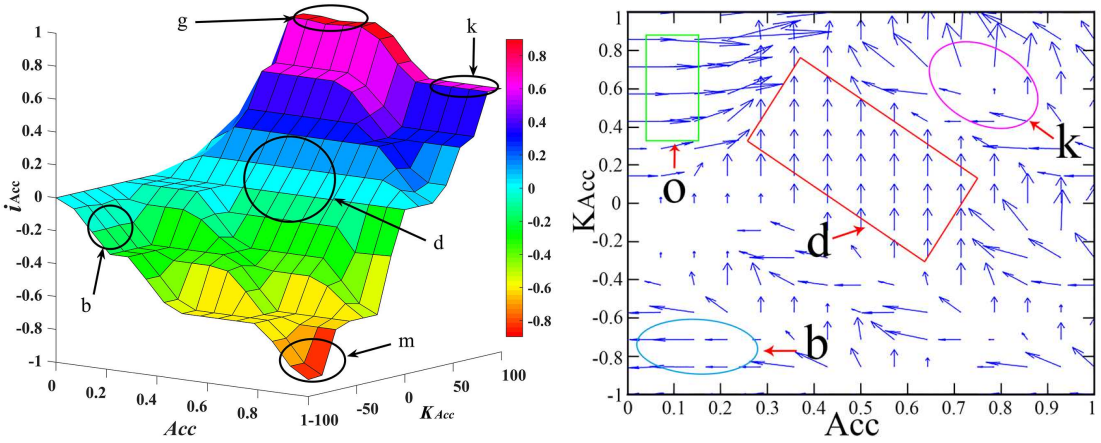

(a) 3D view (b) Vector view

FIGURE 10. Fuzzy inference diagram of torque compensation coefficient

Figure 10(a) is a 3D view and Figure 10(b) is a vector view. The reasoning surface color of Figure 10(a) represents the compensation coefficient value, and the range is $[-1, 1]$. As can be seen from Figure 10(a), according to the established rules, under the same accelerator aperture, the absolute value of the compensation coefficient increases with the increase in the change rate of the accelerator aperture. Region g is the highest point in Figure 10(a). The compensation coefficient corresponds to region f and g in Figure 9(c) at this time. The accelerator aperture is M or B, and the change rate of the accelerator aperture is PB. Region k is slightly lower than region g in Figure 10(a). The change rate of the accelerator aperture is PB. Since the required torque decreases relatively with the increase in speed during acceleration, region k is slightly lower than region g in Figure 10(a). Region m is the lowest point in Figure 10(a). At this time, the accelerator aperture is ZB, and the change rate of the accelerator aperture is NB. The compensation coefficient corresponds to region n in Figure 9(c).

The length of the arrow indicates the magnitude of the required torque in Figure 10(b). The direction of the arrow is the vertical line of the surface in Figure 10(a). The arrow distribution is analyzed as follows. The arrow in region j disperses in three directions. The accelerator aperture is B and the change rate of the accelerator aperture is PM at this time. The compensation coefficient corresponds to region j in Figure 9(c) and corresponds to the area between regions g and k in Figure 10(a) at this time. This shows that the torque requirements in this region are greatly affected by the accelerator aperture and the change rate of the accelerator aperture. The direction of the arrows in region a is to the right, corresponding to the left side of region g in Figure 10(a). The accelerator

opening is ZE or S at this time. The long arrow indicates that the torque requirements are large in this state. It is contradictory to the previous design of no compensation under the small accelerator aperture, but logically it should satisfy the driver's driving needs. The arrow directions of region b are to the left, corresponding to region b in Figure 10(a). The accelerator aperture is S. This is the deceleration state. The arrows of region d are all upward in Figure 10(b), corresponding to region d in Figure 10(a). The accelerator aperture is M. The design rules could satisfy the driver's driving needs by analyzing Figsure 9 and 10.

3.3. **Control Strategy Simulation.** This paper studies the torque control strategy of pure electric buses. It can be seen from the vehicle control logic that the driver controls the throttle pedal opening, and the throttle opening state and the throttle opening change rate signal are fed back to the VCU. The VCU judges whether to compensate the motor torque according to the accelerator aperture. Based on the established rules, if the accelerator aperture is small, the motor output torque does not need to be compensated, but if the accelerator aperture is large, the control algorithm needs to be used to compensate the motor output torque. The optimization process of motor output torque based on fuzzy reasoning is shown in Figure 11. A simulation model of the proposed torque compensation strategy for pure electric buses is built in MATLAB/Simulink. The Simulink simulation model of torque compensation strategy is shown in Figure 12.

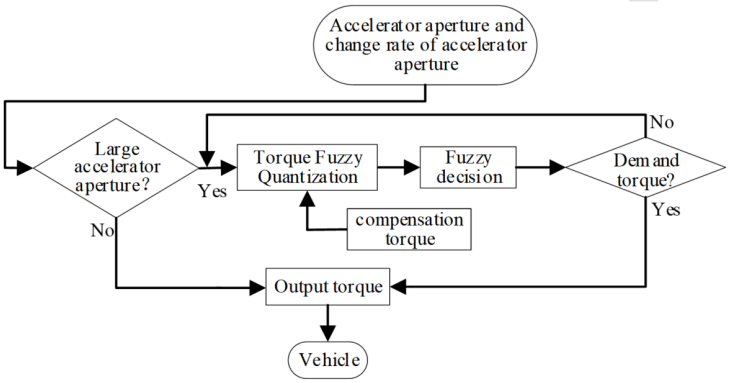

FIGURE 11. Fuzzy reasoning output torque flow

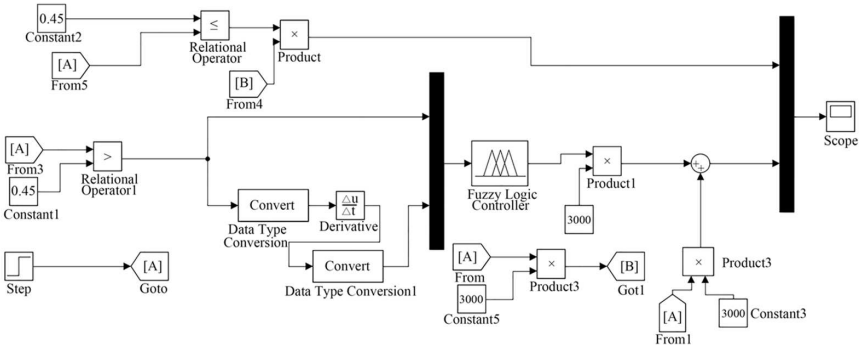

FIGURE 12. The Simulink simulation model of the proposed torque compensation control strategy

Torque compensation control strategy and non-torque compensation control strategy are included in Figure 12. Since the domain of the membership function is defined as

$[0, 1]$, the step function is used as the input to represent the accelerator aperture. The input waveform is shown in Figure 13(a). The abscissa is the time, and the ordinate is the accelerator aperture. The accelerator aperture starts from zero, then the accelerator pedal is controlled to change the accelerator aperture from zero to 100%, and finally the accelerator aperture is kept at 100%. The simulation model is run to obtain the acceleration starting output torque, and the simulation results are shown in Figure 13(b). The purple curve is the output torque result after compensation, and the blue curve is the output torque result when there is no compensation. As shown in Figure 13(b), if the required torque is 3000 $N \cdot m$, the response time with the non-torque compensation strategy is $0.1s$ (point b), and the response time with the torque compensation strategy is $0.0483s$ (point c), so the response time is $0.0517s$ faster (*i.e.*, 51.7% faster) with the torque compensation strategy. When the accelerator aperture is kept constant at 100%, due to the increase in speed, the torque decreases and the torques of the two compensation strategies intersect at point d. Points a and b represent the output torque at 100% accelerator aperture with and without compensation, respectively. Comparing points a and b indicates the torque compensation provided by the torque compensation strategy is 600 $N \cdot m$. To sum up, the proposed torque compensation strategy could improve the output torque. Therefore, the proposed compensation strategy is introduced into a vehicle controller for a real vehicle test.

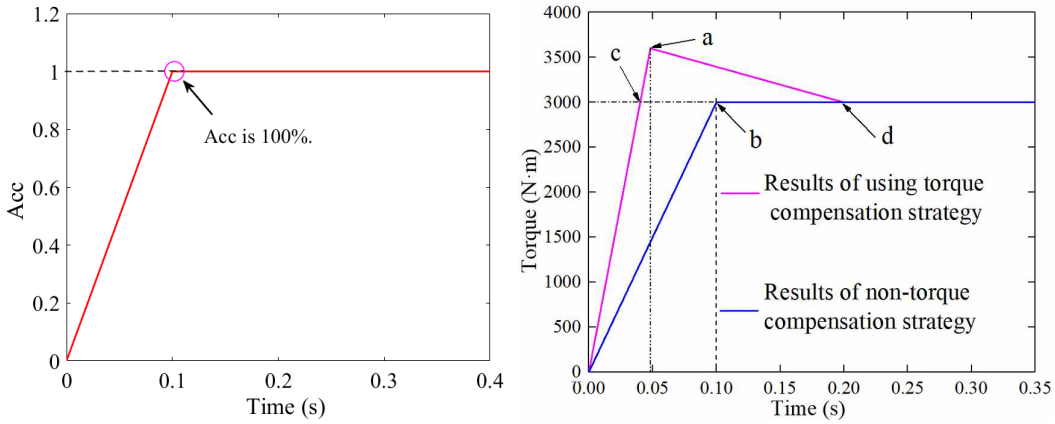

(a) Start of simulation (b) Simulation results

FIGURE 13. The model simulation of torque compensation strategy

4. **Select Drive Motor.** Permanent magnet synchronous motors, DC motors and asynchronous motors are often used in PEVs [32, 33]. A comparison of motor parameters among these three types of motors is shown in Table 2. Permanent magnet synchronous motors have the advantages of high efficiency, small volume, low weight and high reliability. Hence, in this paper, the permanent magnet synchronous motor is chosen to supply motor torque for pure electric buses. The selected permanent magnet synchronous motor is tested, and the efficiency graph and external characteristics of the motor are plotted in MATLAB as shown in Figure 14. From Figure 14(a), it can be seen that the high efficiency range is bounded by the motor speed range of 750-2050 r/min and torque range of 200-1300 $N \cdot m$, and the maximum efficiency reaches 96%. In Figure 14(b), the blue curve is the torque-speed curve, and the red curve is the power-speed curve. The power of the motor increases with the increase in speed, whereas the torque decreases with the increase in speed. Therefore, the upper right portion of Figure 14(a) is a blank area. The area

to the left side of reference line a in Figure 14(b) is the starting area, the area between reference line a and reference line b is the constant torque area, and the area to the right of reference line b is the constant power area. The advantage of using this model is that the motor could still work with high efficiency in the low-speed range as the motor torque increases.

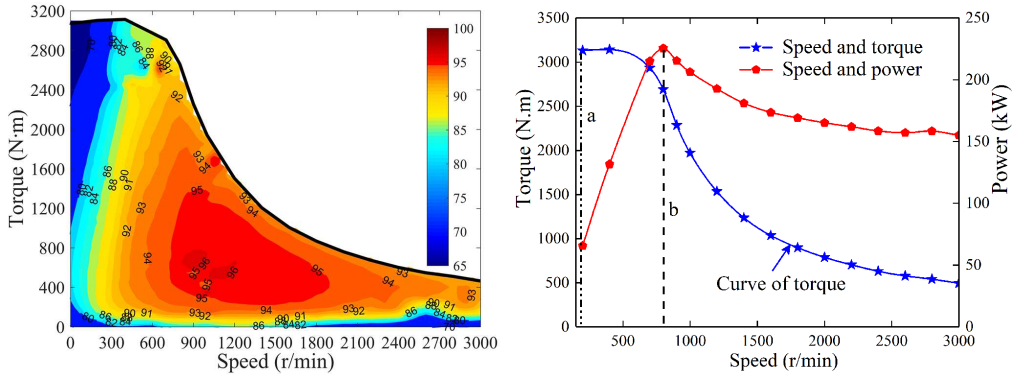

(a) 3D efficiency of torque (b) Characteristic curve of torque

FIGURE 14. Motor test results

TABLE 2. Comparison of motor parameters of three types of motors

Parameter	Permanent magnet synchronous motor	DC motor	Asynchronous motor
Peak efficiency (%)	> 95	85-90	94-95
Speed range	4000-10000	4000-6000	9000-15000
Functional density	high	low	medium
Overload capacity	300	200	300-500
Load efficiency (%)	85-97	80-85	90-92
Motor weight	light	heavy	heavy
Motor size	small	big	heavy
Reliability	excellent	difference	heavy
Maneuverability	good	good	good

5. **Experiment.** It can be seen from the simulation results that the proposed motor torque compensation strategy can increase the motor output torque. To further verify the proposed strategy, the experimental idea is shown in Figure 15. The driver controls the accelerator pedal. The vehicle controller detects the accelerator pedal status and sends the signal to the motor controller. The motor controller operates according to the formulated motor control strategy. The motor status is fed back to the vehicle controller through the motor controller in the form of a message. The computer is connected to the VCU as shown in Figure 16. The VCU, shown in Figure 16(a), is like the brain of the vehicle. Most of the control units on the vehicle are related to the VCU. For example, the battery, motor, gearbox and brake are all controlled by the VCU. The VCU is also the hub for the contact of each control unit. The VCU could realize the functions of acquisition, driving, control, feedback, monitoring and so on. The input line, shown in Figure 16(b), plays a role in connection, as it supplies electricity to the VCU from an electric power source and imports the program from a computer. In addition, the input line includes other cables connected with the vehicle controller. The information input interface of the VCU is shown in Figure 16(c). The corresponding wiring of each unit

is assembled in the interface, and the signal sent by the VCU is sent out through the interface. To verify the rationality and feasibility of the motor torque control strategy design, this paper introduces two control strategies, torque compensation and no torque compensation, into the VCU, and then carries out test verification on the real vehicle. After the test, the whole vehicle control message and the data obtained from the test are analyzed.

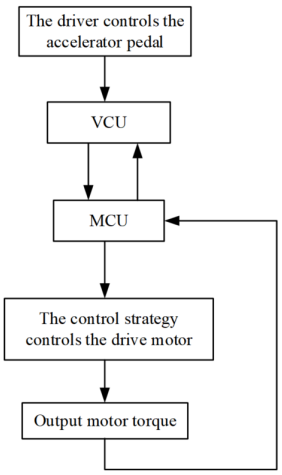

FIGURE 15. Experimental flowchart

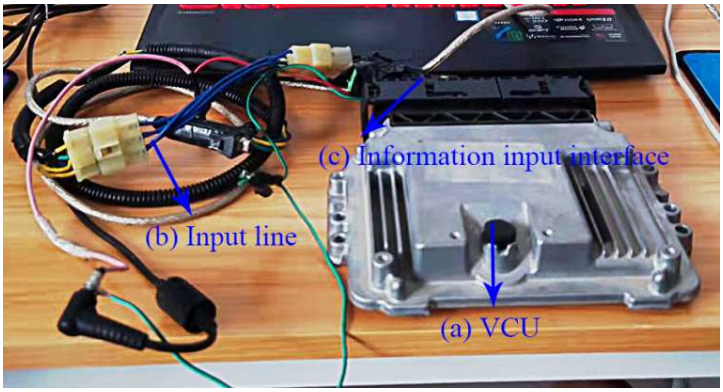

FIGURE 16. Import control strategy into VCU

The experiment takes a pure electric bus as the object. The whole vehicle parameters of the pure electric bus are shown in Table 3. The driver operates the vehicle in different states. The data of accelerator aperture and torque requirements are recorded in real time through CAN message.

After the experiment, the computer is connected with the vehicle controller, the torque is obtained through the computer analysis of the vehicle controller message, and the pedal opening data are added. The accelerator pedal opening and output torque curves are shown in Figure 17. The red dotted line in Figure 17 is the real-time accelerator aperture curve. The black dotted line in Figure 17 is the real-time torque request curve considering torque compensation. The purple curve in Figure 17 is the real-time torque request without considering torque compensation.

It can be seen from Figure 17 that during the $0 - 3.88s$ period, the throttle opening gradually increases at a uniform speed and then remains unchanged. At this time, the

TABLE 3. Whole vehicle parameters of the pure electric bus

Parameter	Value of parameter
Vehicle weight (kg)	12700
Maximum speed (km/h)	100
Rolling resistance coefficient	0.012
Air resistance coefficient	0.65
Frontal area (m^2)	7.1
Wheel rolling radius (m)	0.528
Transmission efficiency	0.93

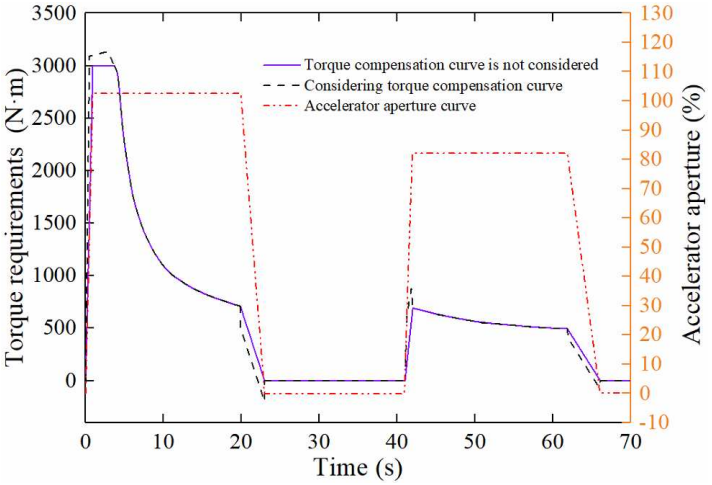

FIGURE 17. Accelerator aperture and torque requirement curve of control strategy of test

torque compensation curve is above the non-torque compensation curve. The starting acceleration state is from 0 to 1.04s. From 1.04s to 3.88s, the accelerator aperture remains unchanged. At 3.88s, the output torques of the two control strategies are the same, which indicates that the developed strategy can increase the output torque to meet the driver's demand for power when starting and accelerating. From 3.88s to 20.02s, the accelerator aperture remains unchanged. At this time, the torque compensation curve and non-torque compensation curve are coincident, and the speed tends to a fixed value. It can be seen from Figure 14(b) that the corresponding torque will decrease as the speed increases, indicating that the driver's demand for speed remains unchanged at this time, which is logical. From 20.02s to 22.91s, the torque compensation curve is under the non-torque compensation. From 22.91s to 40.99s, the torque compensation curve and non-torque compensation curve are coincident. The accelerator aperture is zero and remains unchanged, showing that the vehicle is sliding at this time. From 41.91s to 61.9s, the torque compensation curve and non-torque compensation curve are coincident and the accelerator aperture remains unchanged. From 61.91s to 65.80s, the torque compensation curve is under the non-torque compensation and it is in a deceleration state. From 65.8s to 70s, the torque compensation curve and non-torque compensation curve are coincident and the accelerator aperture is zero. This shows that the vehicle is in a sliding state at this time.

From the experimental data, two curves of torque versus accelerator pedal change rate are obtained, as shown in Figure 18. The blue curve represents the torque without the control strategy, and the red curve represents the torque with the control strategy. To

facilitate analysis, the diagram is divided into six parts. In the first part, the curve with control strategy is above the curve without control strategy. The change rate of accelerator pedal is negative, which means that the driver's control of accelerator pedal opening changes from large to small. At this time, there is little demand for speed. It can be seen from Figure 14(b) that the torque is high when accelerating, so the output torque with control strategy is greater than the output torque without control strategy during rapid deceleration. In the second part, the output torque without control strategy is above the curve with control strategy. The change rate of accelerator pedal opening is still negative, indicating that the accelerator pedal opening decreases and the torque decreases, which is consistent with the established control strategy. In the third part, the change rate of throttle opening is near zero. At this time, the output torque curve without control strategy is close to that with control strategy. The maximum output torque without control strategy is 710.94 $N \cdot m$. The maximum torque output with control strategy is 3120.8 $N \cdot m$, which occurs near the time when the opening of accelerator pedal is constant. In the fourth part, the torque curve with control strategy is above the torque curve without control strategy, and the change rate of accelerator pedal opening is positive, indicating that the accelerator pedal opening increases. According to the formulated rules, the driver needs torque compensation, which is consistent with the control logic. In the fifth part, with the increase of the throttle opening, the output torque curve without control strategy is close to that with control strategy. The minimum output torque without control strategy is 312.12 $N \cdot m$, and the maximum output torque with control strategy is 321.89 $N \cdot m$. This is the torque output at the starting area. The sixth part is similar to the fourth part. The torque curve with control strategy is above the curve without control strategy. The change rate of the accelerator pedal opening is positive, which means that the accelerator pedal opening increases. Since the driver still needs torque, torque compensation is carried out according to the rules.

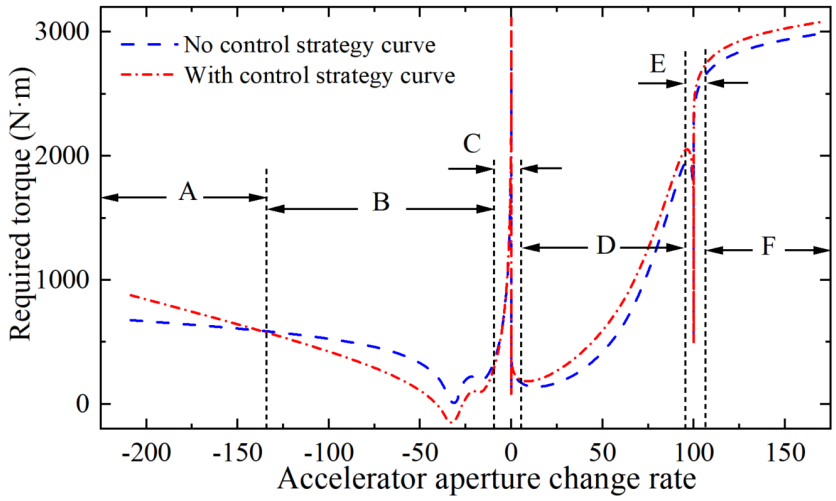

FIGURE 18. Output torque versus accelerator pedal change rate

To sum up, the curves of torque requirement, accelerator pedal opening and output torque versus accelerator pedal opening change rate are obtained from the experimental data. Based on the pedal opening and torque requirement curves in Figure 17, the response speed increases by 44.44% in the starting acceleration stage. During driving, the acceleration response speed increases by 62.86%. In the deceleration stage, the first deceleration response time is shortened by 0.80s, and the second deceleration response time is shortened by 0.62s. Based on the output torque versus pedal opening change rate

curve in Figure 18, according to the formulated motor torque control strategy, the motor output torque with control strategy is greater than that without control strategy at the stage of increasing the accelerator pedal opening. When the accelerator pedal opening decreases, the output torque with control strategy is less than that without control strategy, enabling the motor output torque to meet the driver's demand torque faster. The control strategy could enhance the driver's subjective driving experience and passengers' riding experience.

6. **Conclusion.** A motor torque control strategy is proposed to formulate a control rule to meet the driver's intention, and a pure electric bus is taken as the research object in this paper. Among the three existing kinds of throttle opening determination, the motor output torque is studied using the equal proportion throttle pedal opening. After analyzing the characteristics of different control methods in the control field, fuzzy control is selected. Based on the expert experience method, torque compensation rules are formulated according to the driver's needs. To verify the feasibility of the control strategy, the control strategy model is built in MATLAB/Simulink, and the step function is used as the input. The step function is taken as the input. The simulation results show that the response time of the control strategy increases by 51.7%, and the output torque is increased, indicating that the proposed strategy is feasible.

To further verify the proposed motor control strategy, experiments are conducted on a pure electric bus with permanent magnet synchronous motor both with and without the torque control strategy. The torque requirements, throttle opening, output torque and change rate of throttle pedal opening are obtained. The curves of torque requirement and throttle opening show that the starting acceleration response speed increases by 44.44%. The control strategy with torque compensation could output more torque in a short time. The driving acceleration response speed increases by 62.86%. The deceleration response time also decreases under different accelerator aperture. In other words, the response time of the first deceleration state in the experiment is shortened by $0.80s$. The deceleration response time in the second driving state is shortened by $0.62s$. The response time is reduced. The curves of output torque versus throttle opening change rate show that the output motor torque is consistent with the motor torque compensation, meaning it conforms to the driving intent and can better meet the driver's needs. Therefore, this paper provides a new method for increasing the output torque of pure electric bus motors.

Acknowledgment. This study was funded by Natural Science Foundation of Fujian Province (grant number 2020J01270) and Fujian Industrial Technology Development and Application Project (grant number 2021I0024).

REFERENCES

[1] X.-G. Wu, D.-Y. Zheng, T.-Z. Wang, and J.-Y. Du, "Torque Optimal Allocation Strategy of All-Wheel Drive Electric Vehicle Based on Difference of Efficiency Characteristics between Axis Motors," *Circuits, Systems, and Signal Processing*, vol. 12, no. 6, pp. 1–16, 2019.

[2] W.-Q. Qi, "Fuzzy control strategy of pure electric vehicle based on driving intention recognition," *Journal of Intelligent and Fuzzy Systems*, vol. 39, no. 11, 5131–5139, 2020.

[3] Q.-P. Chen, Z.-H. Li, and W. Peng, "Research on Multi-objective Optimization of Body Stability Controller for Pure Electric Vehicles," *Mechanical and Electrical Engineering*, vol. 35, no. 7, 728–734, 2018.

[4] Y.-P. Zeng, Z.-K. Huang, C. Yang, Y.-G. Liu, Y. Xiao, and Y. Shang, "A Control Strategy for Driving Mode Switches of Plug-in Hybrid Electric Vehicles," *Sustainability*, vol. 10, 1–19, 2018.

[5] J.-G. Ding, and X.-H. Jiao, "A Novel Control Method of Clutch During Mode Transition of Single-Shaft Parallel Hybrid Electric Vehicles," *Electronics*, vol. 9, no. 1, 1–16, 2019.

[6] L. Chen, W. Cheng, and X. Xu, "Optimal control strategy of acceleration output torque of pure electric vehicle based on fuzzy control," *New energy technology*, vol. 4, 56–61, 2015.
[7] Y. Yang, Y.-D. He, Z. Yang, C.-Y. Yang, C.-Y. Fu, and Z.-P. Cong, "Torque Coordination Control of an Electro-Hydraulic Composite Brake System During Mode Switching Based on Braking Intention," *Energies*, vol. 13, no. 8, 1–19, 2020.
[8] L.-J. Xiao, M. Wang, and Z.-H. Zhong, "Shift coordination control and experimental research on two-speed AMT pure electric vehicle," *Journal of Hunan University (Natural Science Edition)*, vol. 46, no. 2, 10–18, 2019.
[9] X. Chen, D. Peng, and Y. Hou, "Research on active control of torsional vibration in pure electric mode of hybrid electric vehicle transmission system," *Mechanical Science and Technology*, vol. 40, no. 7, 1114–1119, 2021.
[10] X.-H. Mo, Y.-Y. Zhu, and H. Yang, "Research on speed control of electric vehicle ramp start motor," *Computer Simulation*, vol. 35, no. 4, 107–111+324, 2018.
[11] Y.-C. Zhang, H.-T. Yang, and B. Xia, "Model predictive torque control of induction motor drives with reduced torque ripple," *Electric Power Applications Iet*, vol. 9, no. 9, 595–604, 2015.
[12] Y.-W. Deng, C.-X. Zheng, and J. Zeng, "Research on Optimal Control of Torque Dynamic Performance of Pure Electric Vehicles," *Computer Simulation*, vol. 34, no. 1, 132–136, 2017.
[13] J. Yang, T.-Z. Zhang, and H.-X. Zhang, "Research on the Starting Acceleration Characteristics of a New Mechanical-Electric-Hydraulic Power Coupling Electric Vehicle," *Energies*, vol. 13, no. 23, 1–20, 2020.
[14] H.-Y. Xiong, Z.-R. Tan, and R.-H. Zhang, "A New Dual Axle Drive Optimization Control Strategy for Electric Vehicles Using Vehicle-to-Infrastructure Communications," *IEEE Transactions on Industrial Informatics*, vol 16, no. 4, 2574–2582, 2020.
[15] G.-B. Sun, Y.-J. Chiu, and G.-W. Lu, "The study of dynamic programming with fuzzy logic energy design and simulation of gear shift for electric vehicles," *Journal of Network Intelligence*, vol. 4, no. 3, 88–99, 2019.
[16] P.-L. Shi, M. Yu, and L. Wei, "Steering stability control strategy of FSAE pure electric racing car based on direct yaw moment control," *Journal of Northwestern University (Natural Science Edition)*, vol. 48, no. 6, 827–837, 2018.
[17] Y.-L. Lei, Y.-X. Zhang, and Y. Fu, "Research on adaptive gearshift decision method based on driving intention recognition," *Advances in Mechanical Engineering*, vol. 10, no. 10, 1–12, 2018.
[18] J.-W. Ju, L.-Z. Bi, and A.-G. Feleke, "Detection of Emergency Braking Intention From Soft Braking and Normal Driving Intentions Using EMG Signals," *IEEE Access*, vol. 9, 131637–131647, 2021.
[19] Y.-Q. Liu, and X.-Y. Wang, "Differences in Driving Intention Transitions Caused by Driver's Emotion Evolutions," *International Journal of Environmental Research and Public Health*, vol. 17, no. 19, 1–22, 2021.
[20] Y.-F. Lian, J.-N. Huang, and S.-S. Liu, "Driving Intention Inference Based on a Deep Neural Network with Dropout Regularization from Adhesion Coefficients in Active Collision Avoidance Control Systems," *Electronics*, vol. 11, no. 15, 4337–4347, 2022.
[21] S.-W. Liu, K. Zheng, and L. Zhao, "A driving intention prediction method based on hidden Markov model for autonomous driving," *Computer Communications*, vol. 157, 143–149, 2020.
[22] Q.-X. Liu, S.-H. Xu, and C. Lu, "Early Recognition of Driving Intention for Lane Change Based on Recurrent Hidden Semi-Markov Model," *IEEE Transactions on Vehicular Technology*, vol. 69, no. 10, 10545–10557, 2020.
[23] Z.-Z. Li, Z.-G. Zhou, and W.-H. Yang, "Regenerative braking control strategy of pure electric vehicle based on braking stability," *Automotive Technology*, vol. 6, 17–23, 2020.
[24] Z.-H. Li, A. Khajepour, and J.-C. Song, "A comprehensive review of the key technologies for pure electric vehicles," *Energy*, vol. 182, 824–839, 2019.
[25] S. Wang, X. Zhao, and Q. Yu, "Research on the control strategy of electric vehicle flat road start based on driver's intention recognition," *Journal of Southwest University (Natural Science Edition)*, vol. 38, no. 12, 140–149, 2016.
[26] W. Liu, H. Qi, and X. Liu, "Evaluation of regenerative braking based on single-pedal control for electric vehicles," *Frontiers of Mechanical Engineering*, vol. 10, 1–14, 2019.
[27] X. Sun, J. Jin, and Y. Cai, "Grey wolf optimization algorithm based state feedback control for a bearingless permanent magnet synchronous machine," *IEEE Trans Power Electron*, vol. 35, 13631–13640, 2020.
[28] Y.-K. Lu, "Adaptive-Fuzzy Control Compensation Design for Direct Adaptive Fuzzy Control," *IEEE Transactions on Fuzzy Systems*, vol. 26, no. 6, 3222–3231, 2018.

[29] M. Alamir, and F. Allgoewer, "Model predictive control," *International Journal of Robust and Nonlinear Control*, vol. 18, no. 8, 799–799, 2008.
[30] F. Liu, "Applying fuzzy logic control to analyze real-time control for charging and discharging power of electric vehicles," *Journal of Intelligent and Fuzzy Systems*, vol. 41, no. 4, 4921–4927, 2021.
[31] B.-M. Keneni, D. Kaur, and A.-A. Bataineh, "Evolving Rule Based Explainable Artificial Intelligence for Unmanned Aerial Vehicles," *IEEE Access*, vol. 25, no. 9, 1–15, 2019.
[32] Z.-H. Li, A. Khajepour, and J. Song, "A comprehensive review of the key technologies for pure electric vehicles," *Energy*, vol. 182, 824–839, 2019.
[33] G.-L. Sun, D.-Y. Sun, and J.-L. Liu, "Performance evaluation and optimization of a novel plug-in power-reflux hybrid electric vehicle powertrain," *International Journal of Energy Research*, vol. 44, no. 5, 3412–3425, 2020.

Appendix A. Fuzzy rule design program. Five subsets of the accelerator aperture and seven subsets of the change rate of the accelerator aperture are formulated in this paper. The torque compensation coefficient comprised the accelerator aperture and the change rate of the accelerator aperture. The rules are defined as follows:

1. If (Acc is ZE) and (K_{Acc} is NB) then (i_{Acc} is ZE)
2. If (Acc is ZE) and (K_{Acc} is NM) then (i_{Acc} is ZE)
3. If (Acc is ZE) and (K_{Acc} is NS) then (i_{Acc} is ZE)
4. If (Acc is ZE) and (K_{Acc} is ZE) then (i_{Acc} is ZE)
5. If (Acc is ZE) and (K_{Acc} is PS) then (i_{Acc} is ZE)
6. If (Acc is ZE) and (K_{Acc} is PM) then (i_{Acc} is ZE)
7. If (Acc is ZE) and (K_{Acc} is PB) then (i_{Acc} is ZE)
8. If (Acc is S) and (K_{Acc} is NB) then (i_{Acc} is NS)
9. If (Acc is S) and (K_{Acc} is NM) then (i_{Acc} is NS)
10. If (Acc is S) and (K_{Acc} is NS) then (i_{Acc} is ZE)
11. If (Acc is S) and (K_{Acc} is ZE) then (i_{Acc} is ZE)
12. If (Acc is S) and (K_{Acc} is PS) then (i_{Acc} is PS)
13. If (Acc is S) and (K_{Acc} is PM) then (i_{Acc} is PM)
14. If (Acc is S) and (K_{Acc} is PB) then (i_{Acc} is PB)
15. If (Acc is M) and (K_{Acc} is NB) then (i_{Acc} is NM)
16. If (Acc is M) and (K_{Acc} is NM) then (i_{Acc} is NS)
17. If (Acc is M) and (K_{Acc} is NS) then (i_{Acc} is NS)
18. If (Acc is M) and (K_{Acc} is ZE) then (i_{Acc} is ZE)
19. If (Acc is M) and (K_{Acc} is PS) then (i_{Acc} is PS)
20. If (Acc is M) and (K_{Acc} is PM) then (i_{Acc} is PM)
21. If (Acc is M) and (K_{Acc} is PB) then (i_{Acc} is PB)
22. If (Acc is B) and (K_{Acc} is NB) then (i_{Acc} is NM)
23. If (Acc is B) and (K_{Acc} is NM) then (i_{Acc} is NM)
24. If (Acc is B) and (K_{Acc} is NS) then (i_{Acc} is NS)
25. If (Acc is B) and (K_{Acc} is ZE) then (i_{Acc} is ZE)
26. If (Acc is B) and (K_{Acc} is PS) then (i_{Acc} is PS)
27. If (Acc is B) and (K_{Acc} is PM) then (i_{Acc} is PS)
28. If (Acc is B) and (K_{Acc} is PB) then (i_{Acc} is PB)
29. If (Acc is ZB) and (K_{Acc} is NB) then (i_{Acc} is NB)
30. If (Acc is ZB) and (K_{Acc} is NM) then (i_{Acc} is NM)
31. If (Acc is ZB) and (K_{Acc} is NS) then (i_{Acc} is NM)
32. If (Acc is ZB) and (K_{Acc} is ZE) then (i_{Acc} is ZE)
33. If (Acc is ZB) and (K_{Acc} is PS) then (i_{Acc} is ZE)
34. If (Acc is ZB) and (K_{Acc} is PM) then (i_{Acc} is PS)
35. If (Acc is ZB) and (K_{Acc} is PB) then (i_{Acc} is PM)